



Published in final edited form as:

Am J Ophthalmol. 2020 February ; 210: 48–58. doi:10.1016/j.ajo.2019.10.022.

Diagnostic Performance of Three-Dimensional Endothelium/Descemet's Membrane Complex Thickness Maps in Active Corneal Graft Rejection

Taher K. Eleiwa^{1,2}, Jane C. Cook¹, Amr S. Elsayy^{1,3}, Vatoorn Roongpoovapatr¹, Vincent Volante¹, Sonia Yoo¹, Mohamed F. Abou Shousha^{1,3,4}

¹Bascom Palmer Eye Institute, Miller School of Medicine, University of Miami, Miami, FL

²Department of Ophthalmology, Faculty of Medicine, Benha University, Egypt

³Electrical and Computer Engineering, University of Miami, Miami, FL.

⁴Biomedical Engineering, University of Miami, Miami, FL.

Abstract

Purpose: To evaluate the performance of three-dimensional (3D) Endothelium/Descemet's membrane complex thickness (En/DMT) maps, versus total corneal thickness (TCT) maps in the diagnosis of active corneal graft rejection.

Design: Cross-sectional study.

Methods: 81 eyes (32 clear grafts and 17 with active rejection, along with 32 age-matched control eyes) were imaged using high-definition optical coherence tomography (HD-OCT), and a custom-built segmentation algorithm was used to generate 3D color-coded maps of TCT and En/DMT of the central 6-mm cornea. Regional En/DMT and TCT were analyzed and compared between the studied groups. Receiver operating characteristic curves were used to determine the accuracy of En/DMT and TCT maps in differentiating between studied groups.

Main Outcome Measures: We evaluated regional En/DMT and TCT.

Results: Both regional TCT and En/DMT were significantly greater in actively rejecting grafts compared to both healthy corneas and clear grafts ($P < 0.001$). Using 3D thickness maps, central, paracentral and peripheral En/DMT achieved 100% sensitivity and 100% specificity in diagnosing actively rejecting grafts (optimal cut-off value, OCV, of 19 μm , 24 μm and 26 μm , respectively), versus only 82% sensitivity and 96% specificity for central TCT, OCV of 587 μm . Moreover, central, paracentral and peripheral En/DMT correlated significantly with graft rejection severity ($r = 0.972$, $r = 0.729$, and $r = 0.823$, respectively; $P < 0.001$).

Conclusion: 3D-En/DMT maps can diagnose active corneal graft rejection with excellent accuracy, sensitivity and specificity. Future longitudinal studies are required to evaluate the predictive and prognostic role of 3D-En/DMT maps in corneal graft rejection.

Keywords

Optical coherence tomography; Descemet's membrane; corneal endothelium; graft rejection

Introduction

Corneal transplantation is the most common type of organ transplantation, with approximately 185,000 corneas transplanted annually in a survey of 116 countries, and 1 in 70 of the needs are covered worldwide.¹ Corneal graft rejection is the leading cause of graft failure in the late postoperative period,^{2,3} and up to 68% of penetrating keratoplasties are affected with at least one episode of rejection.⁴⁻⁷ In full-thickness corneal transplants, graft failure rate secondary to a rejection ranges from 5% in low-risk grafts after five years to 35% in high-risk grafts at three years.⁸ These failures impose a heavy burden on the health care system and on patients' quality of life.⁹ Hence, early detection of graft rejection is crucial to enhance corneal grafts survival and maintain patients' productivity.¹⁰

Clinicians rely on slit-lamp findings of conjunctival injection, corneal edema, epithelial and endothelial rejection lines, sub-epithelial infiltrates, anterior chamber cells and flare, and Descemet folds to diagnose graft rejection,^{7,11} but these findings are only clinically apparent after irreversible loss of endothelial cells has already happened, which are critical for maintenance of corneal transparency.¹² Pachymetry, in-vivo confocal microscopy, specular microscopy and anterior segment optical coherence tomography (AS-OCT) have been investigated to help diagnose a rejection earlier than clinical diagnosis.^{3,13-18} However, these methods analyzed the changes only in the central area of corneal graft and could thus miss an early rejection in the peripheral parts of the corneal graft. In our previous work, we disclosed that manual measurement of central endothelial/Descemet membrane complex thickness (En/DMT) is a novel quantitative index that correlates accurately with the severity of rejection in both ex-vivo and in-vivo studies.¹⁴ Also, we have shown that central En/DMT has better diagnostic performance than endothelial cell density and central corneal thickness in characterizing the immunological status of corneal grafts.^{13,14} However, these measurements were two-dimensional (2D) and thus more susceptible to missing minor changes in the optical scan.

In this study, we compared the performance of three-dimensional (3D) Endothelium/Descemet's membrane complex thickness (En/DMT) maps, versus total corneal thickness (TCT) maps in the diagnosis of active corneal graft rejection. A custom-built segmentation algorithm was used to generate 3D color-coded En/DMT maps from the captured HD-OCT images of the central 6-mm cornea. Compared with manual segmentation, this algorithm has been validated to be capable of segmenting all corneal layers of healthy eyes with similar accuracy, albeit with significantly better repeatability as well as significantly less running-time per image.¹⁹ It utilizes automated segmentation algorithms to generate 3D thickness maps of corneal layers.^{19,23} This quasi-histological visualization can enhance evaluation and diagnosis of various corneal pathologies such as keratoconus,^{24,25} Fuchs' endothelial corneal dystrophy,²⁶ and corneal graft rejection.²⁷ Additionally, we analyzed central, paracentral and peripheral En/DMT parameters that we found highly sensitive and specific

in diagnosing active corneal graft rejection. We also present data demonstrating that regional En/DMT is a much better indicator than central corneal thickness in assessing the immunological status of the corneal graft.

Materials and Methods:

Study population

This study was approved by the University of Miami Institutional Review Board. All participants provided written informed consent before enrollment. The study design followed the tenets of the Declaration of Helsinki for biomedical research.

Forty-nine eyes of 49 patients and 32 eyes of 32 normal controls were prospectively and consecutively recruited from December 2016 to January 2019 at Bascom Palmer Eye Institute, University of Miami. Inclusion criteria for participation included uneventful Penetrating keratoplasty (PK) or Descemet Stripping Automated Endothelial Keratoplasty (DSAEK) surgery performed greater than 1 month prior. Exclusion criteria included corneal grafts with microbial infection or past history of a rejection episode. For the un-operated control eyes, a best corrected visual acuity (BCVA) better than 20/25 on the Snellen scale, and no corneal abnormalities as detected by slit-lamp examination were required to be included in the study. Individuals with recent contact lens use, ocular diseases, previous ocular surgery, and systemic diseases with ocular involvement were excluded. Slit lamp examination was performed on each eye by a masked cornea specialist (either MA or SY) in order to assign the examined cornea into either a clear graft, or actively rejecting category. Active endothelial graft rejection was diagnosed by detecting new keratic precipitates (KPs) or a Khodadoust line in the presence of anterior chamber cells and new persistent corneal graft edema on two consecutive visits in a graft that was previously clear.^{7, 11} Clinical grading corneal grafts rejection based on the ejection severity was not attempted.

Image Acquisition and Analysis

Each participant received anterior segment HD-OCT (Envisu R2210, Bioptigen, Buffalo Grove, IL, USA) with 6 mm radial cuts centered on the corneal vertex. This device uses a super-luminescent diode light source with a central wavelength of 840 nm and it has an axial resolution of 3 μm , and a scanning speed of 32,000 A-scans per second with 36 frames per scan. Each participant was asked to look at a central fixation target and the presence of a visible specular reflection in all images confirmed optimal centration. In decentered grafts and post-PK eyes with high irregular astigmatism, the patient was asked to look at an optimized fixation target to maintain the geometric centration of the scan upon the graft. Custom-built segmentation software was used to segment the corneal epithelium, Descemet's membrane and endothelium automatically with manual editing if needed (Figure 1). Manual editing was executed by two masked operators when the automatic segmentation failed to delineate the irregularities on the endothelial layer in the rejecting corneal grafts. The segmentation software used the Random Sample Consensus (RANSAC) method with a polynomial model to estimate the corneal layer boundaries from potential points obtained from thresholding the OCT image.⁴² Then, the estimates are refined by searching locally in the original image for the best points. The segmentation method is robust to the specular

reflection as each boundary is fitted to a polynomial model which depends on all points and does not get affected that much with the specular reflection, as shown in Figure 1. Then, the segmentation of different frames of the scan is mapped into 3D and interpolated using bi-cubic interpolation to obtain the corneal surfaces. After that, 3D ray tracing is applied iteratively at each interpolated surface to correct for the refraction in the OCT imaging light by applying the vector form of Snell's law at the refractive interface between each 2 successive layers (Figure 2-a).⁴³ Finally, the inter-surface distances are measured as the shortest axial distance between each consecutive surface to generate the thickness maps. We used the refractive index of 1.376 for the corneal layers.⁴⁴ Thickness maps were regionally divided into a central 2 mm circle, surrounded by 2 mm-wide paracentral, and 2 mm-wide peripheral concentric rings (Figure 2-b). The average central, paracentral and peripheral thickness parameters were calculated and used for further analysis. Validation studies of our automated image processing techniques were published in our previous work and the results were comparable to the manual operators.¹⁹

Diagnostic indices

We used three diagnostic indices to describe the regional microstructural characteristics of the En/DM complex; central, paracentral and peripheral En/DMT. We previously reported the 2 interfaces of the En/DM as the two most posterior hyper-reflective bands of the cornea on HD-OCT images.^{14,26}

Statistical Analysis

Statistical analyses were performed using SPSS software version 22.0 (SPSS, Chicago, IL, USA) to calculate descriptive statistics for all eyes. The obtained TCT measurements were verified to have a normal distribution by assessment of histograms and a Shapiro-Wilk's test of normality, while En/DMT was not. Therefore, mean \pm standard deviations (SD) was used to characterize the distribution of the corneal thickness values, while the median values were used to characterize both En/DMT. In addition, one-way analysis of variance (ANOVA) with post-hoc comparisons were performed to account for the differences in central, paracentral, and peripheral corneal thickness, while a Kruskal-Wallis test with pairwise comparisons was used for regional En/DMT. Additionally, factorial-ANOVA was performed to verify if the changes in the corneal thickness and En/DMT depend on the type of graft (Penetrating Keratoplasty; PK versus Descemet Stripping Automated Endothelial Keratoplasty; DSAEK). The sensitivity and specificity of regional En/DMT and regional TCT in differentiating between studied groups were determined by generating receiver operating characteristic curves (ROC). In order to determine if central, paracentral and peripheral En/DMT would be descriptive of graft rejection severity, coefficient of correlation (r-value) of those indices and rejection severity based on central TCT was computed.^{14-16,41} Two-sided p-values less than 0.05 were considered to be statistically significant. Moreover, intraclass correlation coefficients (ICC) were used to assess the inter-operator reliability of the manual measurements in the selected eyes. The ICC is defined as the ratio of the between-subjects variance to the sum of the pooled within-subjects variance and the between-subjects variance.²⁰ The ICC interpretation that was used considered the reliability of the values as poor for values less than 0.2, fair for values from 0.21 to 0.40, moderate for values between

0.41 and 0.60, good for values from 0.61 to 0.80, and excellent for values higher than 0.80.^{21,22}

Results:

Our study included 49 eyes of 49 patients; the breakdown included 32 clear grafts (21 PK and 11 DSAEK), 17 actively rejecting grafts (13 PK and 4 DSAEK), and 32 eyes of 32 age- and gender-matched healthy controls. Table 1 summarizes the different characteristics of all groups. The type of graft (PK versus DSAEK) had no statistically significant effect on the changes in the mean regional corneal thickness and En/DMT values between the studied groups (Figure 3).

Using HD-OCT images, the En/DM in graft rejection was visualized as two smooth hyper-reflective lines with a translucent space in between in both healthy corneas and clear grafts.¹³ In actively rejecting grafts, it appears as a thickened band formed by two hyper-reflective lines with occasional granular hyper-reflectivity (Figure 1). The segmentation software was robust in delineating these granules automatically in most of the eyes except in three cases that needed manual segmentation. Using 3D thickness maps, we were able to quantify both the regional differences in TCT and En/DMT (Figure 4).

Regional analysis of mean central, paracentral, and peripheral En/DMT as well as TCT revealed no statistically significant differences between healthy controls and clear grafts (Table 2). However, there was a statistically significant increase in all parameters in the actively rejecting group compared to healthy eyes and clear grafts ($P < 0.001$). With regards to the evaluation of the inter-operator reliability for the manual measurements, the ICC for TCT was 0.999 (95% Confidence Interval; CI, 0.997–1.00) and the ICC for En/DMT was 0.962 (95% CI: 0.842–0.991).

Table 3 summarizes the diagnostic accuracy of regional TCT, versus En/DMT. Central, paracentral and peripheral En/DMT achieved 100% sensitivity and 100% specificity (optimal cut-off value (OCV) of 19 μm , 24 μm , and 26 μm , respectively), whereas central graft thickness achieved only 88% sensitivity and 90% specificity (OCV of 564 μm) in differentiating actively rejecting grafts from clear grafts (Figure 5).

To test whether central, paracentral and peripheral En/DMT could be used to quantify the severity of graft rejection, we correlated each of them with central corneal thickness as an objective diagnostic index of graft rejection. Central, paracentral and peripheral En/DMTs did not show significant correlations with central corneal thickness in controls and clear grafts. On the other hand, central, paracentral, and peripheral En/DMT of actively rejecting grafts showed a significant linear correlation with central corneal thickness ($r = 0.972$, $P < 0.001$; $r = 0.729$, $P < 0.001$; and $r = 0.823$; $P < 0.001$, respectively; figure 6).

Discussion:

Corneal graft rejection can start as a localized rejection before emanating throughout the entire cornea, hence regional analysis of corneal grafts would provide more substantial results.²⁸ Corneal surgeons depend on clinical signs of limbal injection, aqueous cells,

keratic precipitates in the graft, and segmental or diffuse edema of the graft to diagnose a rejection;^{7,11} however, these findings coincide with permanent endothelial cell injury.¹² This fact highlights the importance of the early and accurate diagnosis of graft rejection to preserve corneal grafts and prolong their survival.^{29–31} Corneal thickness has been used to predict rejection, as increasing central corneal thickness can be a sign of significant endothelial cell dysfunction; however, this is not sensitive for graft rejection.⁵ Decompensation of corneal grafts is usually present before central corneal thickness increases beyond 600 μm .^{32,33} The Cornea Donor Study showed that both central corneal thickness and endothelial cell density were predictive of graft failure from all causes, not only graft rejection.¹⁵

Previous studies had selected the central area of the corneal graft for consistent analysis^{12–18}, which could miss an ongoing rejection in the peripheral parts. Increased central corneal thickness measurements may offer an early warning of rejection, endothelial cell loss, inflammation, or other causes of endothelial cell dysfunction. However, central corneal thickness alone is not a reliable indicator of graft health or decompensation.⁶ The variability of normal corneal thickness between patients also presents a complication, because a mildly thickened graft undergoing rejection may still be within the range of normal.^{6, 15} For instance, acute graft rejection can present early with relatively normal corneal thickness (Figure 4, case 2); meanwhile, thicker grafts do not necessarily indicate active rejection (Figure 4, case 3).

Aqueous humor analysis has been reported to evaluate the increased cytokine levels during rejection of penetrating keratoplasty,³⁴ but it is an invasive means of diagnosing rejection. Contact confocal microscopy has also been studied, and reports show that increased active keratocytes as well as immune cell densities in the central area can diagnose graft rejection via manual counting.^{18,35} Using specular microscopy, Musch et al. reported the significant decrease in the central endothelial cell density in severe graft rejection, whereas mild rejection episodes were not associated with a loss in cell density exceeding the expected.³ Using anterior segment OCT, Abou Shousha et al. reported a higher sensitivity and specificity of central two-dimensional En/DMT in evaluating the immunological status of the corneal graft, versus both central corneal thickness,¹⁰ and endothelial cell density.¹³

Our previous work only used manual measurements to take the 2D thickness measurements in the central region and we were not able to highlight peripheral localized changes that could be signs of an early rejection. In this study, our custom-built segmentation algorithm allows for non-contact in-vivo 3D objective quantification of En/DM complex from images captured using the commercially available anterior segment HD-OCT devices; thus, it is less susceptible to missing minor changes in the optical scan. Briefly, the algorithm works by automatically segmenting all the B-scans, remapping the segmentation into 3D points, interpolating the points to generate the 3D corneal surfaces using bicubic interpolation, correcting the surfaces from light refraction and lastly, measuring the inter-surface distances and subsequently generating the thickness maps.¹⁹ Elsayy A. et al had validated the automatic segmentation of corneal layers using this algorithm, compared to manual operators.¹⁹ Our study reveals excellent inter-operator reliability for the TCT and En/DMT measurements using the manual segmentation for severely distorted corneal layers. Our

current data supports that imaging En/DMT has the highest sensitivity and specificity in diagnosing corneal graft rejection.

In our cross-sectional study, we report that the qualitative and quantitative regional analysis of the En/DM in corneal grafts using 3D color-coded thickness maps can accurately differentiate active rejection from healthy grafts; however, longitudinal studies showing some change in En/DM prior to the occurrence of actual active rejection is still required to validate that this diagnostic tool can detect rejections earlier than the current techniques. En/DM in actively rejecting grafts is characterized by diffuse or sectorial thickening of the posterior hyper-reflective layer with occasional nodular excrescences, giving it a saw-tooth appearance. These hyper-reflective granules may represent a tomographic visualization of the clinically detected KPs. However, the clinical and tomographic chronological changes in the En/DM of actively rejecting grafts were not examined due to the cross-sectional nature of our study. Hence, future longitudinal study is required to correlate the clinically detected KPs with these excrescences seen using OCT, and to evaluate the sensitivity of the 3D thickness maps to detect KPs earlier than slit-lamp examination. Quantitatively, the differences between the central, paracentral and peripheral En/DMT can diagnose acute rejection more accurately than corneal thickness measurements. The contemporaneous increase in the regional En/DMT in active graft rejection may potentially interact with endothelial function and subsequently play a part in the development of graft failure. Further studies are required to evaluate the potential utility of these indices to remotely diagnose corneal graft rejection instead of in office exams. Furthermore, we investigated the objective relationship between the regional En/DMT and central TCT obtained from HD-OCT scans to test whether regional En/DMT could quantify the severity of graft rejection. We found the strongest positive correlation for the central En/DMT, followed by peripheral En/DMT and paracentral En/DMT. Prospective longitudinal study is required to identify the consecutive changes in the En/DMT of corneal allografts and to determine if that correlation could indicate that these changes occur before, and contribute to the edema in the rejecting corneal grafts.

Central En/DMT has been reported to be up to 18 μm in healthy subjects.^{13,14,26,36} Our results in healthy grafts and un-operated corneas match the reported measurements by Pekel et al.³⁷, López de la Fuente et al.³⁸, Alberto et al.³⁹, and Hutchings et al.⁴⁰. Compared to the aforementioned studies, we demonstrated not only the central thickness of En/DM, but also the 3D mapping of the central 6 mm region in healthy corneas, clear grafts, and actively rejecting grafts using our automated segmentation algorithm.

Our study is not without limitations. First, imaging was limited to the central 6 mm of the cornea as the tele-centric probe has diminished axial resolution and signal intensity in peripheral regions. Nevertheless, in the context of keratoplasty, the graft is frequently 1–2.5 mm larger than central 6-mm zone. Second, we used 36 radial cuts on each eye to create a composite three-dimensional model of the cornea. Hence, a noncontiguous model was converted into a contiguous map, which may not account for minor gaps in measurement that may nonetheless be clinically significant. In addition, in severely distorted En/DM, manual editing of the automatically segmented endothelial boundary was necessitated to delineate the irregular excrescences in the En/DM complex. Moreover, the study was not

correlating the clinically graded severity of graft rejection with regional En/DMT indices. However, we used the central TCT as an objective indicator of rejection severity.^{14,16,41} Lastly, the longitudinal changes in En/DMT with progressive corneal allograft rejection weren't examined owing to the cross-sectional nature of this study. Thus, a future prospective longitudinal studies that uses an HD-OCT technology with wider scanning field and a more robust automatic segmentation algorithm are therefore warranted to address the aforementioned limitations and quantify long-term changes in the entire graft to more optimally explore the predictive and prognostic role of En/DMT in corneal graft rejection.

In conclusion, our study has disclosed, for the first time in the literature, the in-vivo 3D color-coded thickness maps of En/DM in corneal grafts. 3D-En/DMT maps have shown excellent sensitivity and specificity in detecting active corneal graft rejection that strongly correlate with the severity of graft rejection. Further studies are required to evaluate the potential utility of 3D-En/DMT maps in prediction and guidance of therapeutic decisions in corneal allograft rejection especially in high-risk corneal transplants.

Acknowledgments / Disclosure:

a. Conflicts of Interest and Source of Funding: Taher Eleiwa, Jane Cook, Amr Elsayy, Vincent Volante and Vatoakarn Roongpoovapatr - None to declare. Sonia Yoo and Mohamed Abou Shousha: United States Non-Provisional Patents (Application No. 8992023 and 61809518), and PCT/US2018/013409. Patents and PCT are owned by University of Miami and licensed to Resolve Ophthalmics, LLC. Mohamed Abou Shousha and Sonia Yoo are equity holders and sit on the Board of Directors for Resolve Ophthalmics, LLC. Sonia H. Yoo is a consultant of CARL Zeiss.

b. Financial Support: This study was supported by a NEI K23 award (K23EY026118), NEI core center grant to the University of Miami (P30 EY014801), and Research to Prevent Blindness (RPB). The funding organization had no role in the design or conduct of this research.

c. Other Acknowledgments: None

d. Declarations:

- 1) Ethics approval and consent to participate: This study was approved by the University of Miami Institutional Review Board.
- 2) Availability of data and material: The datasets used and/or analyzed during the current study available from the corresponding author on reasonable request.
- 3) Authors' contributions: All authors attest that they meet the current ICMJE criteria for Authorship. Each of the coauthors had seen and agreed with each of the changes made to this manuscript in this revision and to the way his or her name is listed.

List of Abbreviations:

En/DM	Endothelium-Descemet's complex
En/DMT	Endothelium-Descemet's complex thickness
TCT	total corneal thickness
HD-OCT	High-definition Optical Coherence Tomography
AS-OCT	Anterior segment Optical Coherence Tomography
ROC	Receiver Operating Characteristics

AUC	Area under curve
OCV	optimal cut-off value
PK	Penetrating keratoplasty
DSAEK	Descemet Stripping Automated Endothelial Keratoplasty
SD	standard deviation
ANOVA	analysis of variance
2D	two-dimensional
3D	three-dimensional
Epi	epithelium
KPs	keratic precipitates

References

1. Gain P, Jullienne R, He Z et al. Global Survey of Corneal Transplantation and Eye Banking. *JAMA Ophthalmol* 2016; 134(2):167–173. [PubMed: 26633035]
2. Wilson SE, Kaufman HE. Graft failure after penetrating keratoplasty. *Surv Ophthalmol* 1990; 34(5): 325–356. [PubMed: 2183380]
3. Musch DC, Schwartz AE, Fitzgerald-Shelton K, Sugar A, Meyer RF. The effect of allograft rejection after penetrating keratoplasty on central endothelial cell density. 1991; 111(6): 739–742.
4. Alldredge OC, Krachmer JH. Clinical types of corneal transplant rejection. Their manifestations, frequency, preoperative correlates, and treatment. *Arch Ophthalmol* 1981; 99(4): 599–604. [PubMed: 7013739]
5. Williams KA, Muehlberg SM, Lewis RF et al. How successful is corneal transplantation? A report from the Australian Corneal Graft Register. *Eye* 1995; 9 (2): 219–227. [PubMed: 7556721]
6. Ing JJ, Ing HH, Nelson LR et al. Ten-year postoperative results of penetrating keratoplasty. *Ophthalmology* 1998; 105(10): 1855–1865. [PubMed: 9787355]
7. Panda A, Vanathi M, Kumar A, Dash Y, Priya S. Corneal graft rejection. *Surv Ophthalmol*. 2007 Jul-Aug 52 (4):375–96 [PubMed: 17574064]
8. Bartels MC, Doxiadis II, Colen TP et al. Long-term outcome in high-risk corneal transplantation and the influence of HLA-A and HLA-B matching. *Cornea* 2003; 22(6):552–6. [PubMed: 12883350]
9. Wilson SE, Kaufman HE. Graft failure after penetrating keratoplasty. *Surv Ophthalmol*, 34 (5) (1990), pp. 325–356 [PubMed: 2183380]
10. Claerhout, Beele H, De Bacquer D et al. Factors influencing the decline in endothelial cell density after corneal allograft rejection. *Invest Ophthalmol Vis Sci* 2003; 44 (11): 4747–6. [PubMed: 14578395]
11. Dua HS, Azuara-Blanco A. Corneal allograft rejection: risk factors, diagnosis, prevention, and treatment. *Indian J Ophthalmol*. 1999, 47(1), 3. [PubMed: 16130277]
12. Lee HS, Kim MS. Influential factors on the survival of endothelial cells after penetrating keratoplasty. *European journal of ophthalmology* 2009, 19(6), 930–935. [PubMed: 19882586]
13. Smith C, Kaitis D, Winegar J. Comparison of endothelial/Descemet's membrane complex thickness with endothelial cell density for the diagnosis of corneal transplant rejection. *Ther Adv Ophthalmol*. 2018 12 3; 1–9.

14. Abou Shousha M, Yoo S, Sayed et al. In vivo characteristics of corneal endothelium/Descemet membrane complex for the diagnosis of corneal graft rejection. *Am J Ophthalmol* 2017; 178: 27–37. [PubMed: 28259779]
15. Verdier DD, Sugar A, Baratz K et al. Corneal thickness as a predictor of corneal transplant outcome. *Cornea* 2013 32(6): 729–36. [PubMed: 23343949]
16. Liu YC, Lwin NC, Chan NS, et al. Use of anterior segment optical coherence tomography to predict corneal graft rejection in small animal models. *Invest Ophthalmol Vis Sci.* 2014; 55: 6736–6741. [PubMed: 25249608]
17. McDonnell PJ, Enger C, Stark WJ, et al. Corneal thickness changes after high-risk penetrating keratoplasty. Collaborative Corneal Transplantation Study Group. *Arch Ophthalmol.* 1993; 111: 1374–1381. [PubMed: 8216018]
18. Chirapapaisan C, Abbouda A, Jamali A et al. In Vivo Confocal Microscopy Demonstrates Increased Immune Cell Densities in Corneal Graft Rejection Correlating with Signs and Symptoms. *Am J Ophthalmol.* 2019, ePublication.
19. Elsayy A, Abdel-Mottaleb M, Sayed I-O, et al. Automatic Segmentation of Corneal Microlayers on Optical Coherence Tomography Images. *Trans. Vis. Sci. Tech* 2019;8(3):39.
20. Koo TK, Li MY. 2016 A guideline of selecting and reporting intraclass correlation coefficients for reliability research. *J Chiropr Med.* 15(2):155–163. [PubMed: 27330520]
21. Lopez de la Fuente C, Sanchez-Cano A, Segura F, Hospital EO, Pinilla I. 2016 Evaluation of total corneal thickness and corneal layers with spectral-domain optical coherence tomography. *J Refract Surg.* 32(1):27–32. [PubMed: 26812711]
22. Koo TK, Li MY. A Guideline of Selecting and Reporting Intraclass Correlation Coefficients for Reliability Research [published correction appears in *J Chiropr Med.* 2017 Dec;16(4):346]. *J Chiropr Med.* 2016;15(2):155–163. [PubMed: 27330520]
23. Abou Shousha M, Elsayy A. U.S. Patent No. US20180192866A1 Washington, DC: Inventor Method and system for three-dimensional thickness mapping of corneal micro-layers and corneal diagnoses. US patent US20180192866A1 (2018).
24. Roongpoovapatr V, Elsayy A, Wen D, et al. Three-Dimensional Bowmans Microlayer Optical Coherence Tomography for the Diagnosis of Subclinical Keratoconus. *Invest Ophthalmol Vis Sci.* 2018; 59(9):5742.
25. Abou Shousha M, Wen D, Yoo SH, et al. Three-Dimensional Corneal Collagen Crosslinking Demarcation Band to Evaluate Corneal Flattening effect from Treatment: Pilot Study. American Academy of Ophthalmology (AAO) Annual Meeting 2017; New Orleans.
26. Abou Shousha MA, Perez VL, Wang J, et al. Use of ultra-high-resolution optical coherence tomography to detect in vivo characteristics of Descemet's membrane in Fuchs' dystrophy. *Ophthalmol.* 2010; 117(6):1220–1227.
27. Roongpoovapatr V, Amr Elsayy A, et al. Diagnosis of Corneal Graft Rejection Using 3-Dimensional Endothelial Descemet Membrane Optical Tomography Poster presented at ASCRS•ASOA Annual Meeting 2018; Walter E. Washington Convention Center.
28. Alldredge OC, Krachmer JH. Clinical Types of Corneal Transplant Rejection Their Manifestations, Frequency, Preoperative Correlates, and Treatment. *JAMA Ophthalmol* 1981; 99(4):599–604.
29. Hill JC, Maske R, and Watson P. Corticosteroids in corneal graft rejection. Oral versus single pulse therapy *Ophthalmology*, 98 (3) (1991), pp. 329–333. [PubMed: 2023754]
30. Yamazoe K, Shimazaki-Den S, Shimazaki J. Prognostic factors for corneal graft recovery after severe corneal graft rejection following penetrating keratoplasty *BMC Ophthalmol*, 13 (2013), p. 5. [PubMed: 23432898]
31. Claeihout H, Beele D, De Bacquer P. Kestelyn Factors influencing the decline in endothelial cell density after corneal allograft rejection *Invest Ophthalmol Vis Sci*, 44 (11) (2003), pp. 4747–4752. [PubMed: 14578395]
32. Afshari NA, Pittard AB, Siddiqui A, et al. Clinical study of Fuchs corneal endothelial dystrophy leading to penetrating keratoplasty: a 30-year experience. *Arch Ophthalmol.* 2006; 124: 777–780. [PubMed: 16769829]

33. Seitzman GD, Gottsch JD, Stark WJ. Cataract surgery in patients with Fuchs' corneal dystrophy: expanding recommendations for cataract surgery without simultaneous keratoplasty. *Ophthalmology*. 2005; 112: 441–446. [PubMed: 15745771]
34. Maier P, Heizmann U, Böhringer D. Predicting the risk for corneal graft rejection by aqueous humor analysis. *Mol Vis*. 2011 4 25; 17:1016–23. [PubMed: 21541263]
35. Kocaba V, Colica C, Rabilloud M et al. Predicting Corneal Graft Rejection by Confocal Microscopy. *Cornea* 2015 10; 34 Suppl 10:S61–4. [PubMed: 26252743]
36. Bizheva K, Haines L, Mason E, et al. In Vivo Imaging and Morphometry of the Human Pre-Descemet's Layer and Endothelium with Ultrahigh-Resolution Optical Coherence Tomography. *Invest Ophthalmol Vis Sci*. 2016; 57(6):2782–2787. [PubMed: 27206248]
37. Pekel G, Yagc R, Acer S, Ongun GT, Çetin EN, Simavl H. Comparison of Corneal Layers and Anterior Sclera in Emmetropic and Myopic Eyes. 2015; 34(7):786–790.
38. Lopez de la Fuente C, Sanchez-Cano A, Segura F, Hospital EO, Pinilla I. Evaluation of Total Corneal Thickness and Corneal Layers With Spectral-Domain Optical Coherence Tomography. *J Refract Surg*. 2016; 32(1):27–32. [PubMed: 26812711]
39. Alberto D, Garello R. Corneal Sublayers Thickness Estimation Obtained by High-Resolution FD-OCT. *Int J Biomed Imaging*. 2013; 2013:989624. [PubMed: 23818895]
40. Hutchings N, Simpson TL, Hyun C, et al. Swelling of the Human Cornea Revealed by High-Speed, Ultrahigh-Resolution Optical Coherence Tomography. *Invest. Ophthalmol. Vis. Sci* 2010; 51(9): 4579–4584. [PubMed: 20435597]
41. Flynn TH, Ohbayashi M, Dawson M et al. Use of ultrasonic pachymetry for measurement of changes in corneal thickness in mouse corneal transplant rejection. *Br J Ophthalmol*. 2010; 94(3): 368–71. [PubMed: 19822919]
42. Fischler MA, & Bolles RC Random sample consensus: a paradigm for model fitting with applications to image analysis and automated cartography. *Communications of the ACM*, 1981; 24(6), 381–395.
43. Artal P *Handbook of Visual Optics, Two-Volume Set*: CRC Press; 2017.
44. Yadav R, Kottaiyan R, Ahmad K, Yoon G-Y. Epithelium and Bowman's layer thickness and light scatter in keratoconic cornea evaluated using ultrahigh resolution optical coherence tomography. *J Biomed Opt* 2012; 17:116010. [PubMed: 23117805]

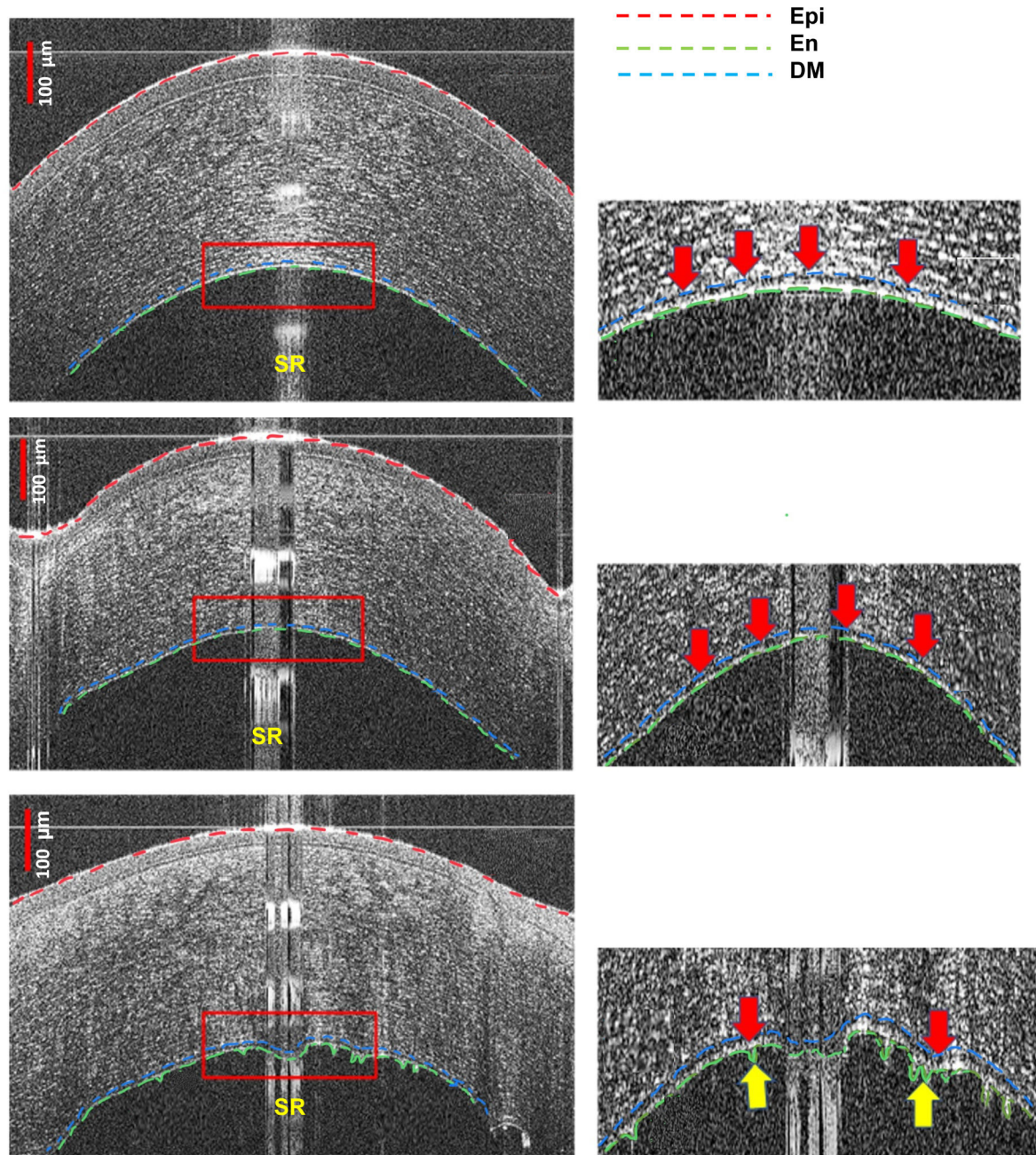


Figure 1: High-definition optical coherence tomography (HD-OCT) images of a healthy unoperated cornea (First row, left), clear corneal graft (Second row, left) and an actively rejecting graft (Third row, left). Presets (Right column) show magnified images of the posterior part of the corresponding cornea on the left. The red dashed line represents the anterior boundary of the corneal epithelium (Epi), the green dashed line indicates the corneal endothelium (En), and the blue dashed line for Descemet’s membrane (DM). In the presets, the thick arrows indicate the segmentation of the endothelium/Descemet’s membrane complex (En/DM). Endothelium/Descemet’s membrane complex thickness (En/DMT) is measured as the inter-

surface distance between the segmented En and DM layers. The specular reflection (SR) confirmed optimal centration, however, the segmentation method is robust, as each boundary is fitted to a polynomial model, and thus does not get affected that much. In both healthy corneas and clear grafts, corneal En and DM were visualized as a band formed by 2 smooth hyper-reflective lines with a translucent space in between (First and second rows, right). In actively rejecting grafts (third row), En/DM appeared as a thickened band bounded by 2 hyper-reflective lines. The anterior line and the translucent space in between the lines were like those of the healthy corneas and clear grafts, while the posterior line had a broader hyper-reflectivity (third row, right) and occasional nodular excrescences (third row, right, yellow arrows). Bars are 100 μm .

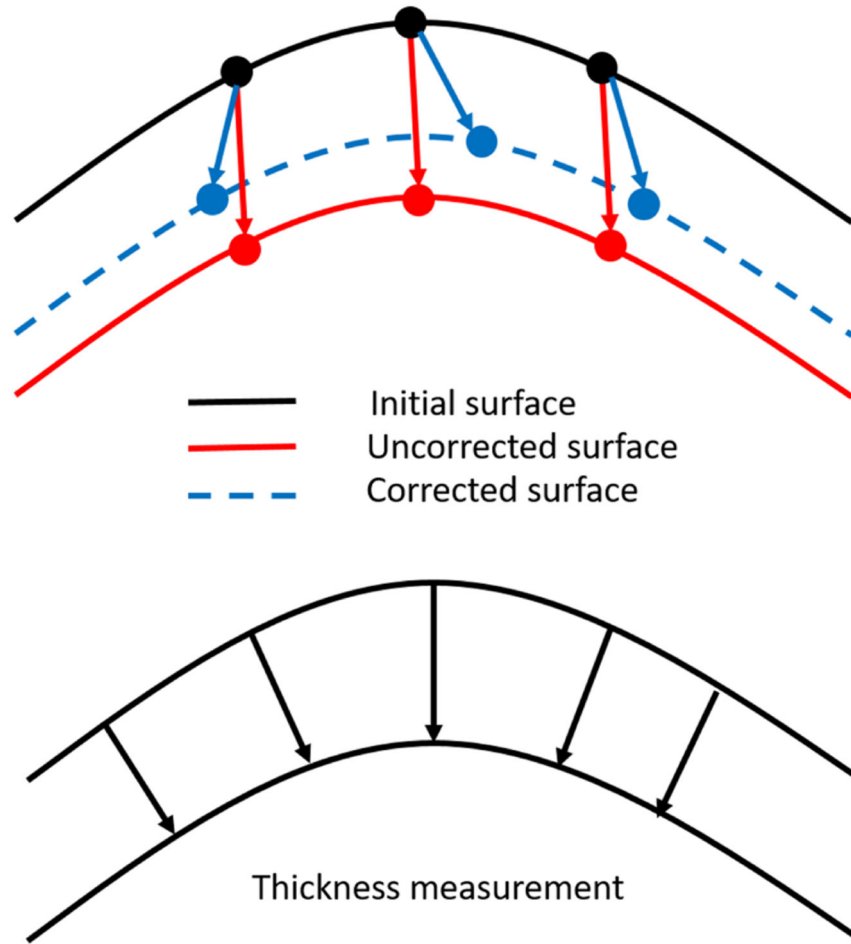


Figure 2-a: A diagram showing the concept of thickness measurement using three-dimensional ray tracing. The axial distances between the uncorrected surfaces (red arrows) represent the optical path length and it is converted to geometric distance (blue arrows) using the layer refractive index. Three-dimensional ray tracing is applied iteratively at each surface to correct for the refraction in the OCT imaging light by applying the vector form of Snell’s law at the refractive interface between each 2 successive layers. Then, the thickness is measured as the shortest distance (black arrows) between each consecutive surfaces.

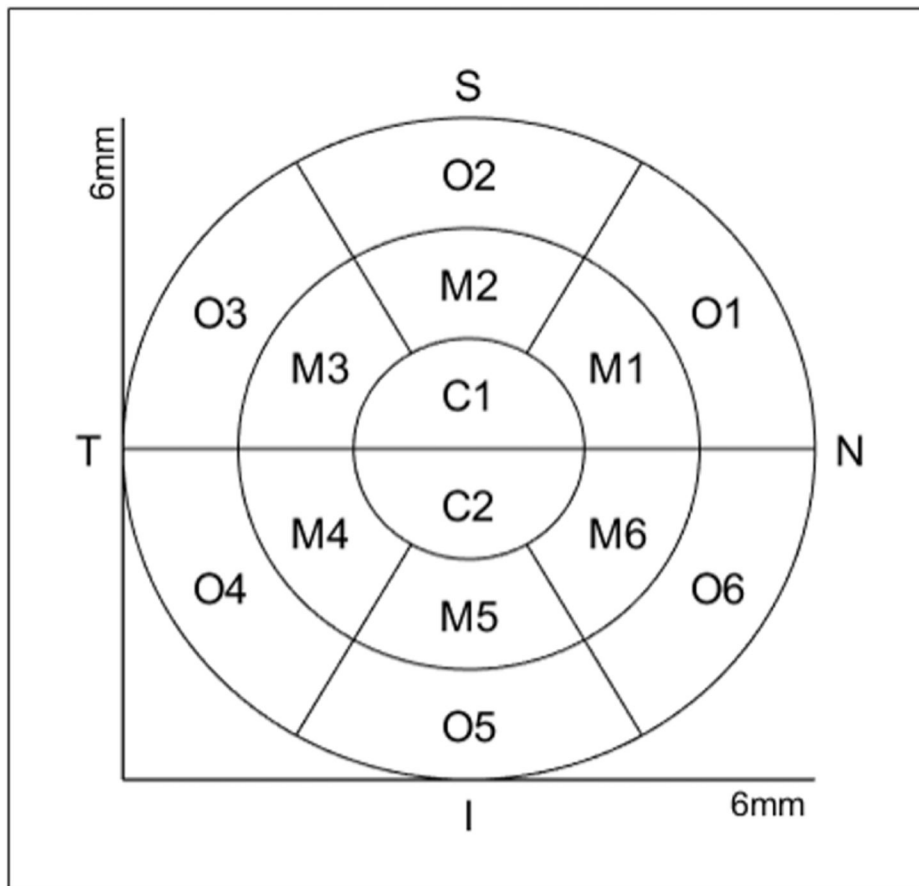


Figure 2-b:
 The scheme of arrangement of the corneal regions for quantitative evaluation of the layer thickness: Central region (C1, C2) lies within a 1 mm radius, surrounded by 2 concentric paracentral (M1, M2, M3, M4, M5, M6) and outer (O1, O2, O3, O4, O5, O6) rings, each with a 2 mm width. N: Nasal; S: Superior; T: Temporal; I: Inferior.

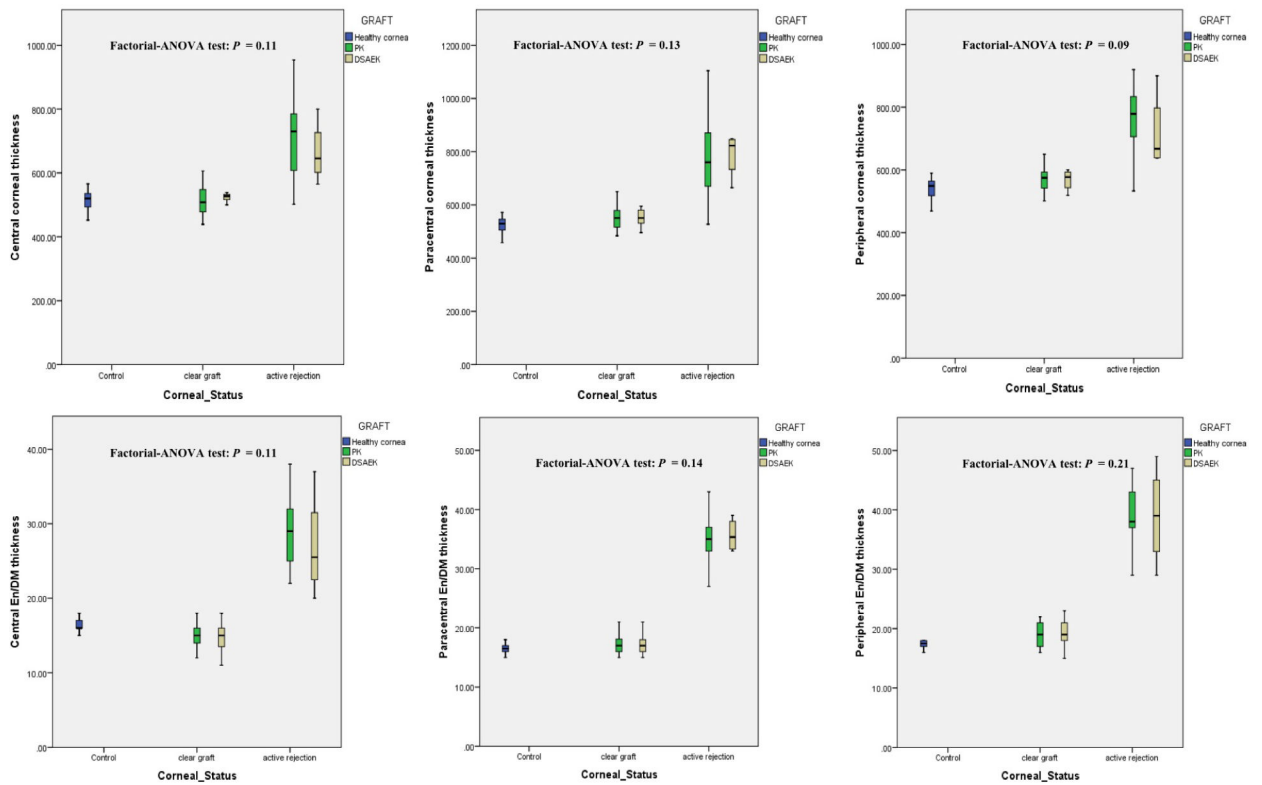


Figure 3: Box-plot distributions showing that there was no statistically significant effect of the type of graft-Penetrating keratoplasty (PK) versus Descemet Stripping Automated Endothelial Keratoplasty (DSAEK)-on the changes in the mean central, paracentral and peripheral total corneal thickness (upper row), and central, paracentral and peripheral endothelium/ Descemet’s membrane complex (En/DM) thickness (lower row) values between the studied groups.

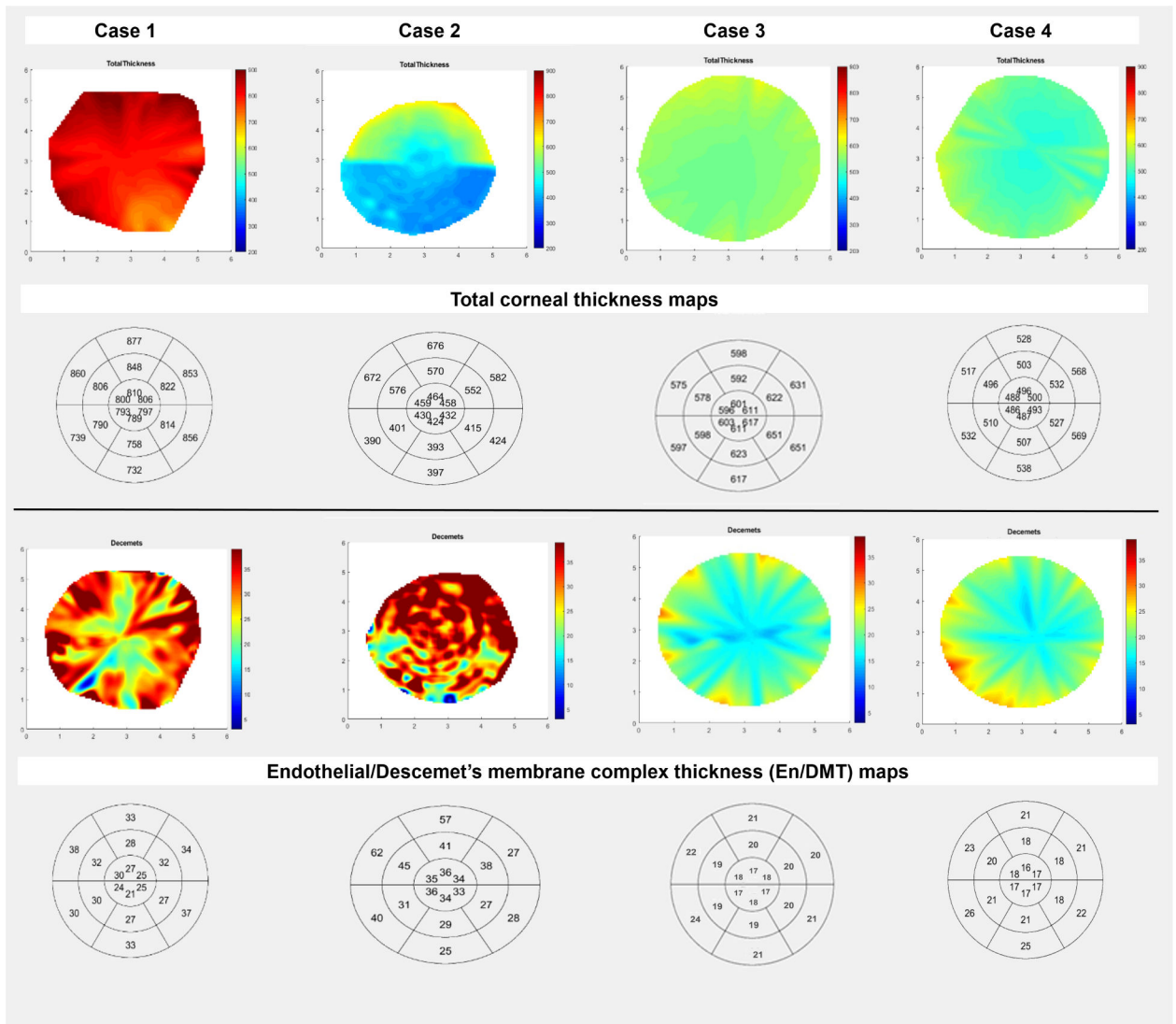
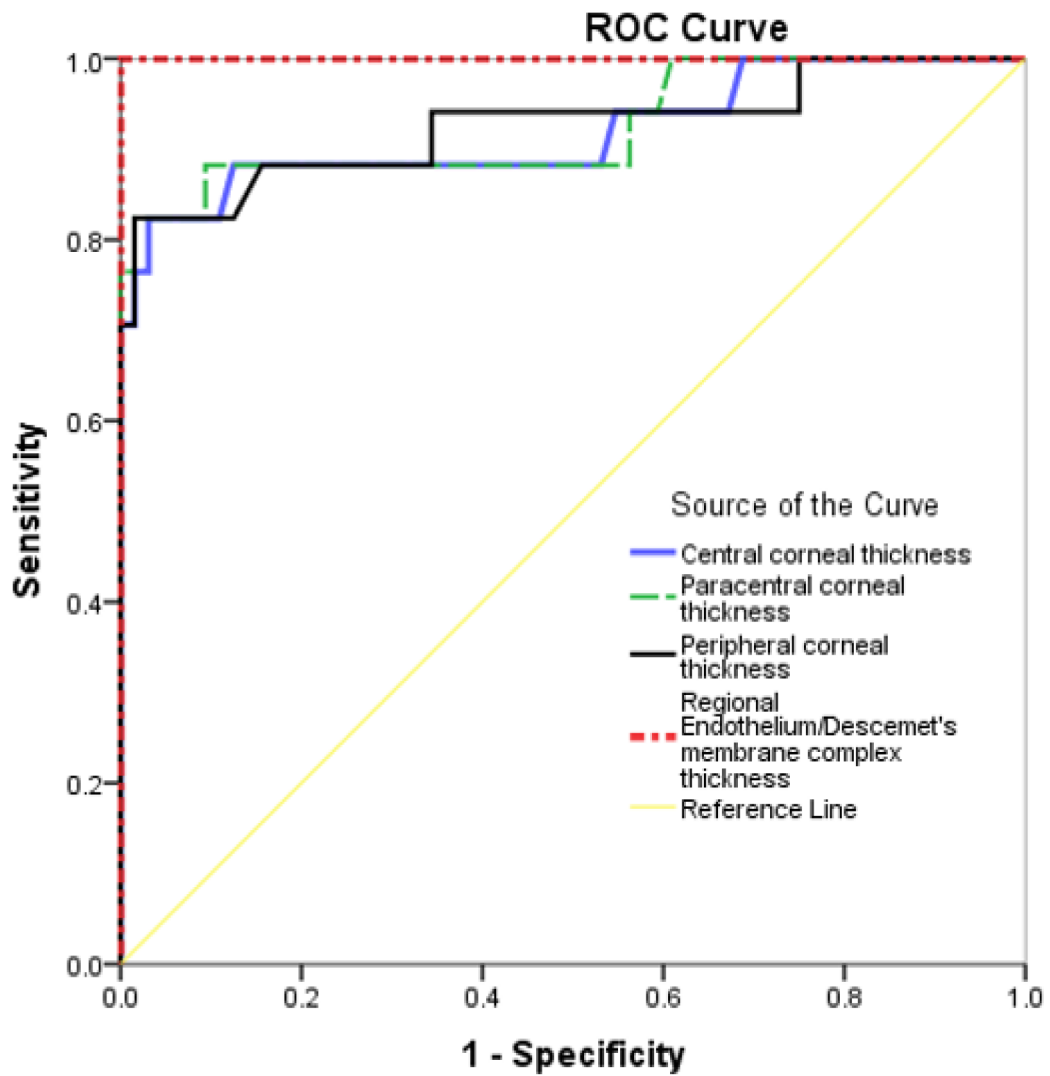


Figure 4: Graph showing the discrimination between two actively rejecting corneal grafts (case 1 and case 2), a clear corneal graft (case 3) and healthy unoperated cornea (case 4) using color-coded and bulls-eye three-dimensional thickness maps of the total corneal thickness (TCT, 1st and 2nd rows) and endothelial/Descemet’s membrane complex thickness (En/DMT, 3rd and 4th rows). En/DMT was higher in case 1 and 2 compared to case 3 and 4. Interestingly, case 2 showed an active rejection in a thin corneal graft with high En/DMT compared to a healthy thicker graft (case 3) with normal En/DMT. Note the striking difference between the presented cases using the self-explanatory color-coded En/DMT maps.



Diagonal segments are produced by ties.

Figure 5: Combined receiver operating characteristics (ROC) graphs of central, paracentral and peripheral corneal thickness; regional endothelial/Descemet's membrane complex thickness (En/DMT) in differentiating clear corneas from actively rejecting grafts. Regional En/DMT provided excellent discrimination (area under the curve, AUC, 1), whereas the central, paracentral and peripheral corneal thickness achieved an AUC of 0.922, 0.926 and 0.926, respectively.

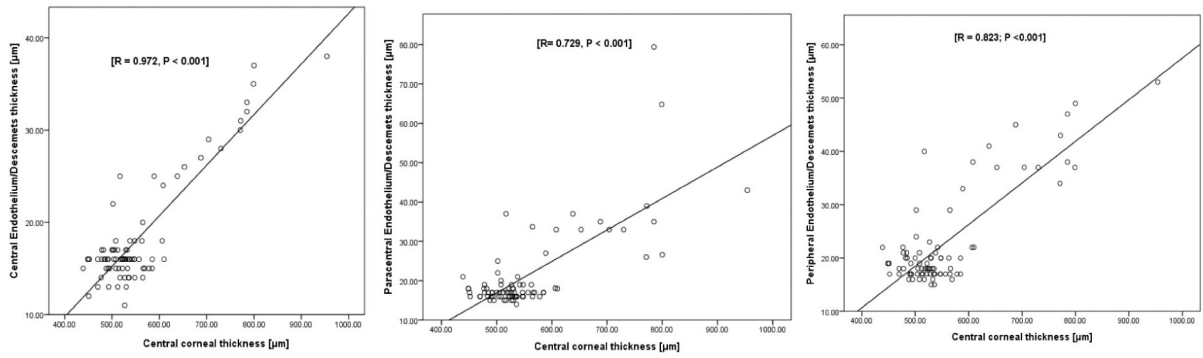


Figure 6: Scatter plots showing a significant linear correlation between central corneal thickness and regional endothelial/Descemet's membrane complex thickness (En/DMT) values in actively rejecting grafts.

Table 1:

Characteristics of our study groups

		Healthy control	Clear grafts	Actively rejecting grafts	<i>p</i> value
Number of eyes	Unoperated cornea	32	—	—	—
	PK	—	21	13	
	DSAEK	—	11	4	
Gender	Female	14	13	10	<i>p</i> = 0.06**
	Male	18	19	7	
Age (years)		46±18	56±18	59±22	<i>p</i> = 0.06**
Postoperative time (Months)		—	8±5	10±4	<i>p</i> = 0.11**
Central corneal thickness (µm)		516±28	518±39	697±119	<i>p</i> <0.001**
Paracentral corneal thickness (µm)		527±27	552±41	766±149	<i>p</i> <0.001**
Peripheral corneal thickness (µm)		543±29	569±37	744±119	<i>p</i> <0.001**
Central DMT (µm)*		16	15	28	<i>p</i> <0.001***
Paracentral DMT (µm)*		17	17	35	<i>p</i> <0.001***
Peripheral DMT (µm)*		18	19	38	<i>p</i> <0.001***

DMT: Endothelial/Descemet membrane complex (En/DM) thickness; PK: Penetrating keratoplasty; DSAEK: Descemet Stripping Automated Endothelial Keratoplasty Values are presented as means ± standard deviation.

DMT is presented as median values.

**
p value is generated using one-way ANOVA test.

p value is generated using Kruskal-Wallis test.

Author Manuscript

Author Manuscript

Author Manuscript

Author Manuscript

Table 2:

Pairwise comparisons of central, paracentral and peripheral Endothelial/Descemet thickness (En/DMT), and total corneal thickness (TCT) means in studied groups.

Dependent Variable	(I) Studied groups	(J) Studied groups	Mean Difference (I-J), μm	Standard Error	P value	95% Confidence Interval	
						Upper Bound	Lower Bound
Central corneal thickness	control	Clear graft	-2	15	0.993	-38	35
		Active rejection	-181 *	18	0.000	-225	-136
	Clear graft	Active rejection	-179 *	18	0.000	-223	-134
Paracentral corneal thickness	control	Clear graft	-25	18	0.376	-69	19
		Active rejection	-239 *	22	0.000	-292	-186
	Clear graft	Active rejection	-214 *	22	0.000	-267	-161
Peripheral corneal thickness	control	Clear graft	-25	15	0.222	-62	10
		Active rejection	-201 *	18	0.000	-245	-157
	Clear graft	Active rejection	-175 *	18	0.000	-219	-131
Central En/DMT	control	clear graft	1	0.6	0.223	-0.5	2
		Active rejection	-12 *	0.7	0.000	-14	-10
	Clear graft	Active brejection	-13 *	0.7	0.000	-15	-11
Paracentral En/DMT	control	Clear graft	-1	0.5	0.249	-2	0.4
		Active rejection	-18 *	0.6	0.000	-19	-16
	Clear graft	Active rejection	-17 *	0.6	0.000	-18	-15
Peripheral En/DMT	control	Clear graft	-2	0.7	0.056	-3	-0.9
		Active rejection	-21 *	0.9	0.000	-23	-19
	Clear graft	Active rejection	-20 *	0.9	0.000	-21.6752	-17.4167

*The mean difference is significant at the 0.05 level.

Receiver operating characteristic (ROC) curve data which represent the diagnostic performance of regional En/DMT, and regional total corneal thickness (TCT) in diagnosing actively rejecting corneal grafts.

Table 3:

	Central TCT	Paracentral TCT	Peripheral TCT	Central En/DMT	Paracentral En/DMT	Peripheral En/DMT
P value	<0.001	<0.001	<0.001	<0.001	<0.001	<0.001
AUC	0.922	0.926	0.926	1.0	1.0	1.0
Sensitivity	88%	88%	88%	100%	100%	100%
Specificity	90%	90%	84%	100%	100%	100%
Cutoff value	564 µm	583 µm	592 µm	19 µm	24 µm	26 µm

AUC = area under the curve; En/DMT= endothelial/Descemet thickness; TCT= total corneal thickness. Specificity, sensitivity, and cutoff values are chosen to maximize total diagnostic accuracy (minimize total number of errors).